International Journal of Computational Intelligence Systems, Vol. 8, Supplement 2 (2015), 16-27

Gray Scale Edge Detection using Interval-Valued Fuzzy Relations

Agustina Bouchet [1,2] , Pelayo Quirós [3] , Pedro Alonso [3] , Virginia Ballarin [1] , Irene Díaz [4] , Susana Montes [5]

[1] *Digital Image Processing Group, Engineering Faculty, National University of Mar del Plata*
Avenida de Juan B. Busto 4302,
Mar del Plata, 7600, Argentina
E-mail: {abouchet,vballari}@fi.mdp.edu.ar
[2] *CONICET,*
Argentina
[3] *Department of Mathematics, University of Oviedo,*
Calle Luis Ortiz Berrocal s/n, Campus de Viesques,
Gijón, Asturias, Spain
E-mail: {uo205956, palonso}@uniovi.es
[4] *Department of Computer Science, University of Oviedo,*
Calle Jesús Arias de Velasco s/n,
Oviedo, Asturias, Spain
E-mail: sirene@uniovi.es
[5] *Department of Statistics and O. R. University of Oviedo,*
Calle Luis Ortiz Berrocal s/n, Campus de Viesques,
Gijón, Asturias, Spain
E-mail: montes@uniovi.es

Received 28 July 2015

Accepted 30 October 2015

Abstract

Gray scale edge detection can be modeled using Fuzzy Sets and, in particular, Interval-Valued Fuzzy Sets. This work is focused on studying the performance of several Interval-Valued Fuzzy Sets construction methods for detecting edges in a gray scale image. These construction methods are based on considering information related to the neighborhood of each point. Thus, several construction methods are proposed and tested, showing the approach performing better.

Keywords: Interval-Valued Fuzzy Sets, Lower Constructor, Upper Constructor, Edge detection, Fuzzy Mathematical Morphology.

1. Introduction

Edge detection plays an important role in the field of binary, grayscale or colour image processing. An edge is defined as a set of connected pixels that lie on a particular boundary between two regions. Edges characterize object boundaries and are useful for segmentation, feature extraction, and identification of objects in an image. Edges are mainly understood as the lack of continuity in an image. Therefore, edge detection refers to the process of locating discontinuities in an image [1].

There are many different approaches to edge detection with the aim to extract contour features. Classical edge detectors are based on a discrete differential operator [2], derivatives [3] or wavelet transformations [4], among others.

In addition, there are several approaches to edge detection based on statistical inference. In this case edge detection is data driven instead of model based [5]. However, the performance of most of these classical methods degrades with noise. In this context, Mathematical Morphology (MM) provides an alternative approach to image processing based on concepts of set theory, topology, geometry and algebra [6,7,8]. The basis of MM is to compare the objects of interest with a set of predefined and known geometry, called Structuring Element. In addition, edge detection depends on the shape and size of this structuring element. Fuzzy Mathematical Morphology (FMM) [9] has emerged as an extension of the MM's binary operators to gray level images, by redefining the set operations as fuzzy set operations, based on the theory of Fuzzy Sets (FS) [10]. It is inspired by the observation that both greyscale images and FS are modeled as mappings from a universe into the unit interval [0,1].

On the other hand, it is well known that some construction methods associated to the so called Interval-Valued Fuzzy Sets (IVFSs) are very useful in detecting edges in gray scale images [11, 12 ,13]. IVFSs [14] are based on generalizing the membership function as a closed interval in $[0,1]$. They present a huge number of applications to many different domains [15].

The aim of this paper is to compare different image edge detection methods based on a construction method for Interval-Valued Fuzzy Relations (IVFR). It is a natural approach as in edge detection is necessary to take into account the influence of neighboring data on the data itself.

The remainder of the paper is structured as follows. Section 2 revises basic concepts related to IVFSs. Section 3 describes basic concepts regarding the construction of Interval-Valued Fuzzy Relations. In Section 4 the weighted construction method for IVFR is presented. Section 5 establishes the relation between IVFR and edge detection. Finally, Section 6 draws some experiments and Section 7 the main conclusion of this work are highlighted.

2. Interval-Valued Fuzzy Sets

IVFS [14] are extensions of classical Fuzzy Sets (FS) [16]. A FS is defined by a function μ that maps each element $x \in X$ onto a value $\mu(x) \in [0,1]$. In contrast, an IVFS is defined as follows

Definition 2.1 *An IVFS in the finite set X, A, is defined by the membership function:*

$$A : X \to L([0,1]).$$

$L([0,1])$ *denotes the set of all closed subintervals of* $[0,1]$*:*

$$L([0,1]) = \{[a_l, a_u] | (a_l, a_u) \in [0,1]^2 \text{ and } a_l \leqslant a_u\}.$$

Fuzzy Relations (FR) generalize the notion of relations in the same way as fuzzy sets generalize the concept of set. While a crisp relation represents the presence or absence of interconnectedness between the elements of two sets, FR allow different degrees or strengths between elements. These degrees are represented by membership grades in a FR in the same way as degrees of set membership are represented in a fuzzy set. FR are defined as follows.

Definition 2.2 *Let X and Y be two finite sets. Each* $R : X \times Y \to [0,1]$ *defines a FR.*

FR are extended to Interval-Valued Fuzzy Relations (IVFRs) as follows.

Definition 2.3 *Let X and Y be two finite sets. An IVFR R is defined by the membership function* $R : X \times Y \to L([0,1])$.

An IVFR can be denoted by

$$R = \{((x,y), R(x,y)) | x \in X, y \in Y\}, \qquad (1)$$

where $R(x,y)$ is the degree of strength of the relation between x and y represented by an interval.

Let $X = \{0,1,\ldots,P-1\}$ and $Y = \{0,1,\ldots,Q-1\}$ be two finite universes, then the FRs are described by matrices in the following way

$$R = \begin{pmatrix} R(0,0) & R(0,1) & \cdots & R(0,Q-1) \\ R(1,0) & R(1,1) & \cdots & R(1,Q-1) \\ \cdots & \cdots & \cdots & \cdots \\ R(P-1,0) & R(P-1,1) & \cdots & R(P-1,Q-1) \end{pmatrix}.$$

3. Construction of IVFR

A way to construct an IVFR is to consider the membership degree of an element as an interval representing the variation between the membership degrees of such element and its neighbors in the original FR[11]. This construction method is briefly described in this section.

The IVFR construction method is based on two constructors (called lower and upper constructors) in order to obtain the limits of each interval. In addition, it involves t-norms and t-conorms [17,18] which are well known generalizations of conjunction and disjunctions in classical logic. Definitions 3.1, 3.2 and 3.3 establish the basic method to construct an IVFR.

According to [11], the basic method to construct an IVFR from a FR is to associate an interval to each element of the initial relation. In order to generate the lower and upper bounds of each interval, the concepts of lower and upper constructors are introduced as follows.

Definition 3.1 *Consider $X = \{0,1,\ldots,P-1\}$ and $Y = \{0,1,\ldots,Q-1\}$ two universes, $R \in F(X\times Y)$ a FR, two t-norms T_1, T_2, two t-conorms S_1, S_2, and $n,m \in \mathbb{N}$ such that $n \leqslant \frac{P-1}{2}$ and $m \leqslant \frac{Q-1}{2}$. Then,*

- *$L^{n,m}_{T_1,T_2} : F(X\times Y) \to F(X\times Y)$ is the lower constructor associated to T_1, T_2, n and m. It is defined by:*

$$L^{n,m}_{T_1,T_2}[R](x,y) = \underset{\substack{i=-n\\ j=-m}}{\overset{m}{\underset{}{\overset{n}{T_1}}}} \left(T_2(R(x-i,y-j),R(x,y))\right), \quad (2)$$

- *$U^{n,m}_{S_1,S_2} : F(X\times Y) \to F(X\times Y)$ is the upper constructor associated to S_1, S_2, n and m. It is defined by*

$$U^{n,m}_{S_1,S_2}[R](x,y) = \underset{\substack{i=-n\\ j=-m}}{\overset{m}{\underset{}{\overset{n}{S_1}}}} \left(S_2(R(x-i,y-j),R(x,y))\right), \quad (3)$$

$\forall (x,y) \in X\times Y$, where i, j take values such that $0 \leqslant x-i \leqslant P-1$ and $0 \leqslant y-j \leqslant Q-1$.

The neighborhood considered to construct the IVFR is represented by a $(2n+1)\times(2m+1)$ matrix. In addition, $\overset{n}{\underset{i=1}{T}} x_i = T(x_1,\ldots,x_n)$.

From lower and upper constructors the IVFR relation is constructed as the following definition states.

Definition 3.2 *Consider $R \in F(X\times Y)$ be a FR, $L^{n,m}_{T_1,T_2}[R]$ a lower constructor and $U^{n,m}_{S_1,S_2}[R]$ an upper constructor, then $R^{n,m}$ is defined by:*

$$R^{n,m}(x,y) = [L^{n,m}_{T_1,T_2}[R](x,y), U^{n,m}_{S_1,S_2}[R](x,y)], \quad (4)$$

for all $(x,y) \in X\times Y$ is an IVFR from X to Y.

The last step is to obtain another FR from the IVFR obtained according to Definition 3.2.

Definition 3.3 *Let $L^{n,m}_{T_1,T_2}[R]$ be a lower constructor and let $U^{n,m}_{S_1,S_2}[R]$ be an upper constructor, them the W-fuzzy relation associated to them is obtained by:*

$$W[R^{n,m}](x,y) = U^{n,m}_{S_1,S_2}[R](x,y) - L^{n,m}_{T_1,T_2}[R](x,y). \quad (5)$$

As it can be deduced from previous definitions, both lower and upper constructors depend on t-norms and t-conorms and on the shape and size of the considered vicinity. In [11] it is analyzed the effect of using different t-norms and t-conorms and different sizes of the submatrix defining the neighborhood (different values for n and m) around each element of a FR on the IVFR.

4. Weighted construction of IVFR

In the method developed in [11], the lower and upper constructors are obtained taking into account that the influence of all the elements in the considered vicinity is the same.

However, it makes sense to think that the influence of an element closer to an element should be higher than the influence of other farther element in the vicinity. In this section we try to model this fact.

In other words, our goal is to obtain the final lower and upper constructors as a combination of lower and upper constructors in such a way that the smaller constructors have more strength[13]. This procedure is introduced in the following definition.

Definition 4.1 *Given two finite universes of natural numbers $X = \{0,1,\ldots,P-1\}$ and $Y = \{0,1,\ldots,Q-1\}$, $R \in FR(X,Y)$ a fuzzy relation in $X \times Y$, two t-norms T_1, T_2, two t-conorms S_1, S_2, and $n,m \in \mathbb{N}$ such that $n \leqslant \frac{P-1}{2}$ and $m \leqslant \frac{Q-1}{2}$, for any $i = 1,2\ldots,\max(n,m)$ we can consider the two fuzzy relations $L^i[R]$ and $U^i[R]$ defined by*

$$L^i[R](x,y) = L_{T_1,T_2}^{\min(i,n),\min(i,m)}[R](x,y) \tag{6}$$

and

$$U^i[R](x,y) = U_{S_1,S_2}^{\min(i,n),\min(i,m)}[R](x,y) \tag{7}$$

In the next step these values are weighted in an appropriate way. Thus, the final lower and upper constructors associated to any fuzzy relation $R \in FR(X \times Y)$ are obtained as follows:

$$L[R](x,y) = \sum_{i=1}^{k} w_i L^i[R](x,y) \tag{8}$$

and

$$U[R](x,y) = \sum_{i=1}^{k} w_i U^i[R](x,y), \tag{9}$$

where k denotes the maximum of n and m.

Finally, it is necessary to determine the weights w_i such that they satisfy $w_i \geqslant w_{i+1}$, so the smaller neighborhoods have more strength. The weights proposed in this paper are based on assigning a different value to each point in the neighborhoods. We have considered three cases:

- Average of the k neighborhoods:

$$w_i = \frac{1}{k}, \quad i = 1,\ldots,k,\ w_i \in (0,1). \tag{10}$$

- An equidistant version of the weights with a constant increase given by the next restrictions:

$$\begin{cases} \sum_{i=1}^{k} w_i = 1, \\ w_i \in (0,1), & i = 1,\ldots,k, \\ w_i - w_{i+1} = C, & i = 1,\ldots,k-1, \\ w_k = C, \end{cases} \tag{11}$$

where $C \in (0,1)$ is a constant. With some calculation [13], the expression of the weights is

$$w_i = \frac{2(k-i+1)}{k(k+1)}, \quad i = 1,\ldots,k. \tag{12}$$

- A constant relation between two consecutive weights, given $N \in \mathbb{N}\backslash\{1\}$:

$$\begin{cases} \sum_{i=1}^{k} w_i = 1, \\ w_i \in (0,1), & i = 1,\ldots,k, \\ w_i / w_{i+1} = N, & i = 1,\ldots,k-1, \\ w_k = C, \end{cases} \tag{13}$$

where $C \in (0,1)$ is a constant. From these conditions it follows than $w_i = N^{k-i}C$ for all i. Thus, after some calculations [13], the expression of the weights is reached as follows:

$$w_i = N^{k-i}\frac{N-1}{N^k-1},\ i = 1,\ldots,k. \tag{14}$$

Note that the bigger the value of N, the greater the importance on the central pixels. Moreover, note that the case $N = 1$ is not considered, because in that case the weights are selected according to the average of the k neighborhoods method.

Once the values of the weights are calculated, and therefore, both lower and upper constructors, the remaining steps of the method in Section 3 (Definitions 3.2 and 3.3) must be applied in order to get the new IVFR and the W-fuzzy relation.

It should be noted that the fact of using weights cause the appearance of some values very close to 0 or 1, but not the own value. The reason is that the use of the biggest neighborhoods can make a little influence in such value. To avoid this situation, a smoothing step is used such that the final W-fuzzy edge image W is modified with some cut point $\alpha \in (0,0.5)$.

Given W a fuzzy relation, the smoothing step with cut point $\alpha \in (0, 0.5)$ is carried out as follows:

1. If $W(x,y) < \alpha$, then $W^\alpha(x,y) = 0$.
2. If $W(x,y) > 1 - \alpha$, then $W^\alpha(x,y) = 1$.
3. For the remaining values in the closed interval $[\alpha, 1-\alpha]$, they are expanded to the closed interval $[0,1]$ keeping the original proportion:

$$W(x,y) \to W^\alpha(x,y) = 0.5 + \frac{1}{1-2\alpha}(W(x,y) - 0.5). \quad (15)$$

The reason to take values in the interval $(0, 0.5)$ lies in the fact that when $\alpha \to 0$, the smoothing step leads us to the method without such step, as sets of points modified by parts 1 and 2 of it tends to the empty set. Meanwhile, the remaining values get the modification:

$$W^\alpha(x,y) \xrightarrow[\alpha \to 0]{} 0.5 + (W(x,y) - 0.5) = W(x,y). \quad (16)$$

If the value α where greater or equal to 0.5, it would make no sense to apply the smoothing step, as there would be pixels whose value must be changed to 0 (step 1) and to 1 (step 2) at the same time.

The scheme of the weighted method [13] with the smoothing step receives as input a fuzzy relation $R \in FR(X,Y)$, the dimensions of the neighborhood to construct the upper and lower constructors ($n, m \in \mathbb{N}$), two t-norms, two t-conorms and the value of α. It produces as output a W-fuzzy relation, $W^\alpha \in FR(X,Y)$. The algorithm applies Definition 4.1 to compute each $L^i[R]$ and $U^i[R]$ and conputes w_i for each $i \in 1, \ldots, max(n,m)$. Finally, it constructs $R^{n,m}_{T_1,T_2,S_1,S_2}$ from L and U according to Definition 3.2. W is then computed from this $R^{n,m}_{T_1,T_2,S_1,S_2}$ (see Definition 3.3). The last step computes W^α from W.

In the experimentation carried out in the next section, the influence of α, along with the comparison of this new approach with the non-weighted one are analyzed with a grey scale database.

5. IVFR and Fuzzy Mathematical Morphology

In this section it is studied how the IVFR construction methods can be used in gray image edge detection problems and the link between IVFR and FMM.

The main objective of the MM is to extract information of the geometry and topology of an unknown set in an image. The key of this methodology is the Structuring Element, a small set completely defined with a known geometry, which is compared to the whole image[7]. FMM combines MM and fuzzy set theory to extend the applicability of this model by adding the ability to handle uncertainty [19, 20, 21, 22, 23].

Thus, both the images and the structuring elements are represented as fuzzy sets. The following definition states what a gray scale image is in terms of a fuzzy set.

Definition 5.1 *A gray scale image μ whose dimensions are $P \times Q$ pixels, is a FR where the finite sets used are $X = \{0, 1, \ldots, P-1\}$ and $Y = \{0, 1, \ldots, Q-1\}$.*

The definition of the structuring element ν is straightforward as it is a restriction of an image to a set of pixels. Then basic operators are defined as follows.

Definition 5.2 *([21,24]) Let μ be a gray scale image and let ν be an structuring element. Then the Fuzzy Morphological Dilation and Fuzzy Morphological Erosion of the image μ by the SE ν are defined respectively as:*

$$\delta(\mu,\nu)(x) = sup_{y \in U}[t(\mu(y), \nu(y-x))],$$

$$\varepsilon(\mu,\nu)(x) = inf_{y \in U}[s(\mu(y), c(\nu(y-x)))],$$

where $t(a,b)$ is a t-norm, $s(a,b)$ is a t-conorm and $c(a) = 1-a$ is the fuzzy complement operator.

Gradient operators are used in segmentation because they enhance intensity variations in image. These variations are assumed to be edges of objects. This is why gradients are also called "edge detectors". They are presented in the following definition.

Therefore, a gray image μ is represented as a FR. At the same time it is possible to obtain an IVFR from a FR. Therefore, it is also possible to construct edge detectors that can be understood as gradient operators from a MM point of view. Let's introduce the concept of morphological gradient.

Definition 5.3 *([21,7]) Let μ be a gray scale image and let ν be an SE, then*

- *The basic morphological gradient of the image μ by the SE ν is:*

$$Grad_{D,E}(\mu,\nu) = \delta(\mu,\nu) - \varepsilon(\mu,\nu).$$

- *Internal gradient of the image μ by the SE ν is:*

$$Grad_{E}(\mu,\nu) = \mu - \varepsilon(\mu,\nu).$$

- *External gradient of the image μ by the SE ν is:*

$$Grad_{D}(\mu,\nu) = \delta(\mu,\nu) - \mu.$$

Gradient by erosion detects edges in the positions of lower gray levels in the edges while Gradient by dilation detects edges in the positions of higher gray levels in the edges. In addition, the morphological gradient grouped the results of these two operators, getting thicker contours.

On the other hand, as gray scale images can be represented by FRs according to Definition 5.1, from the outputs produced by the IVFR construction method we can define three different edge operators using these constructors. These constructors represent the three gradients afore and are defined as follows

Definition 5.4 *Consider a gray scale image μ and the structuring element defined by n and m, then the following gradients can be defined:*

- *Gradient:*

$$R^{n,m} = U^{n,m}_{S_M,S_P} - L^{n,m}_{T_M,T_P}. \qquad (17)$$

- *Internal Gradient (obtained from Lower Constructor):*

$$\mu - L^{n,m}_{T_M,T_P}. \qquad (18)$$

- *External Gradient (obtained from Upper Constructor:*

$$U^{n,m}_{S_M,S_P} - \mu. \qquad (19)$$

Figure 1 shows the effect of the gradient, internal and external gradients on an image.

Note that the image obtained from the lower constructor (the internal gradient) represents a darker version of the original image. Depending on the t-norms chosen, this image can be more or less dark. Depending on the pair of t-norms selected, different lower constructors are obtained. Figure 2 shows the effect of different t-norms on the lower constructor. When the minimum t-norm is applied ($T_M = T_1 = T_2$ in Equation 6), the image obtained by the lower constructor is shown in the top-right part of Figure 2. Note that the edges are well defined in this case. When $T_1 = T_P$ (product t-norm) and $T_2 = T_M$ the image obtained by the lower construction is darker than the original one (bottom-left image). When $T_1 = T_2 = T_P$ the lower constructor produces a almost a black image, being the darkest one (bottom-right figure) .

On the other hand, the image produced by the upper constructor represents a brighter version of the original image. As for the lower constructor, depending on the $t-conorms$ this image can be more or less bright. Figure 3 shows the effect of different t-conorms on the upper constructor. When the maximum t-conorm is applied ($S_M = S_1 = S_2$ in Equation 7), the image obtained by the upper constructor is shown in the top-right part of Figure 3. Note that the edges are well defined in this case and the image is brighter than the original one. When $S_1 = S_P$ (probabilistic sum) and $S_2 = S_M$ the image obtained by the upper construction is brighter than both the original one and the obtained with the maximum t-conorm (bottom-left image). When $S_1 = S_2 = S_P$ the upper constructor produces a almost a white image, being the brightest one (bottom-right figure) .

Finally, the W-fuzzy edge image represents the difference of contrast between both constructors. The edges can be identified in this image. Figure 4 shows and example of a W-fuzzy image using $S_1 = S_M$, $S_2 = S_P$, $T_1 = T_M$ and $T_1 = T_P$.

6. Experiments

The W-fuzzy image as well as the edge images produced by both lower and upper constructors can be

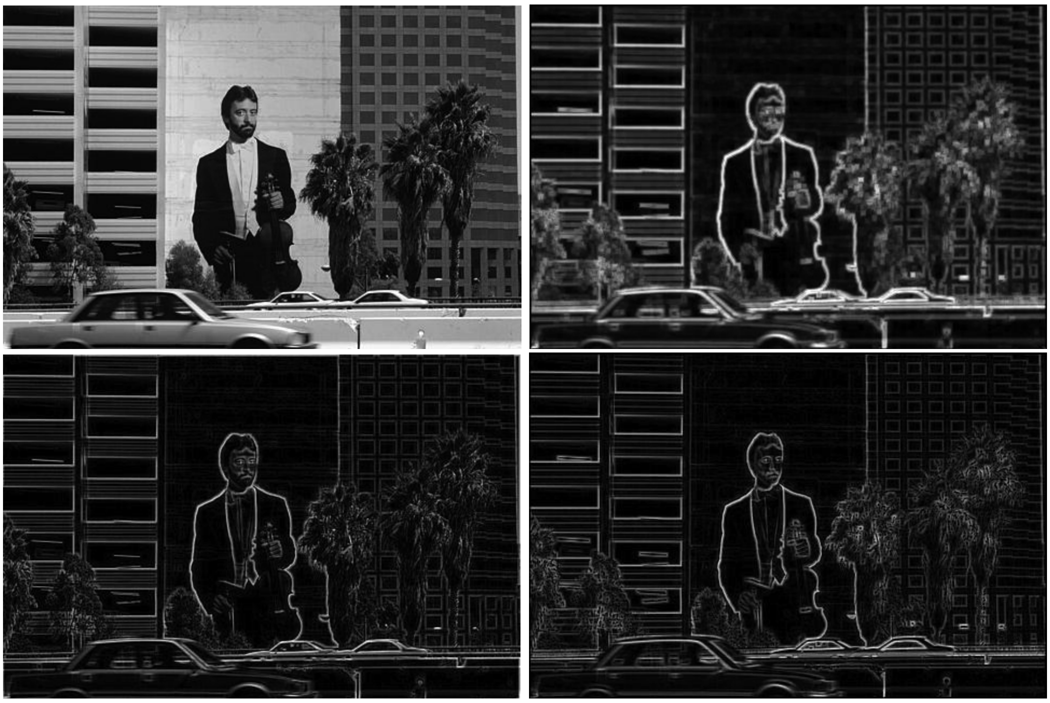

Figure 1: Original image (top left), gradient (top right), internal gradient (bottom left) and external gradient (bottom top).

powerful tools in detecting edges for gray scale images.

The goal of this section is to compare the edge images obtained by lower and upper constructors and also the W-fuzzy one.

To make such experimentation, the *Berkeley Segmentation Dataset* [25] is used. This database contains original images and its corresponding edge images. The first 25 images from the test set were selected, whose dimensions are 481×321 (or 321×481) pixels.

The comparison is performed in terms of the least squares estimator by comparing respectively the image produced by the lower constructor, the upper constructor and the W-fuzzy image to ideal image obtained from the dataset. In addition, the t-norms and t-conorms are the standard ones (Minimum-Maximum).

In addition, as the behavior of weighted methods against non weighted are studied in [13], we restrict ourselves to the comparison among the three edge images (the obtained from lower, upper constructors and the fuzzy image) depending on the considered parameters.

Therefore the different configurations analyzed for the weighting methods are:

- **Methods to obtain weights:** average (A), equidistant method (E) and constant relation method with (C) $N = 2,3,4,5$ (II, III, IV, V).
- **Number of neighborhoods:** $k = 2$, $k = 3$ or $k = 4$ (2,3,4).
- **Smoothing step parameter value:** $\alpha \in \{0, 0.05, 0.1, \ldots, 0.4, 0.45\}$.

Figure 5 compares the performance in detecting edges of the internal gradient (lower constructor) with different weighting methods.

Left part of Figure 5 shows the performance of the fuzzy image (that is, the gradient) in detecting edges when two neighborhoods are considered. In the same way, graphs at the middle (right) part of Figure 5 represent the performance of the fuzzy image in detecting edges when three (four) neighborhoods are considered.

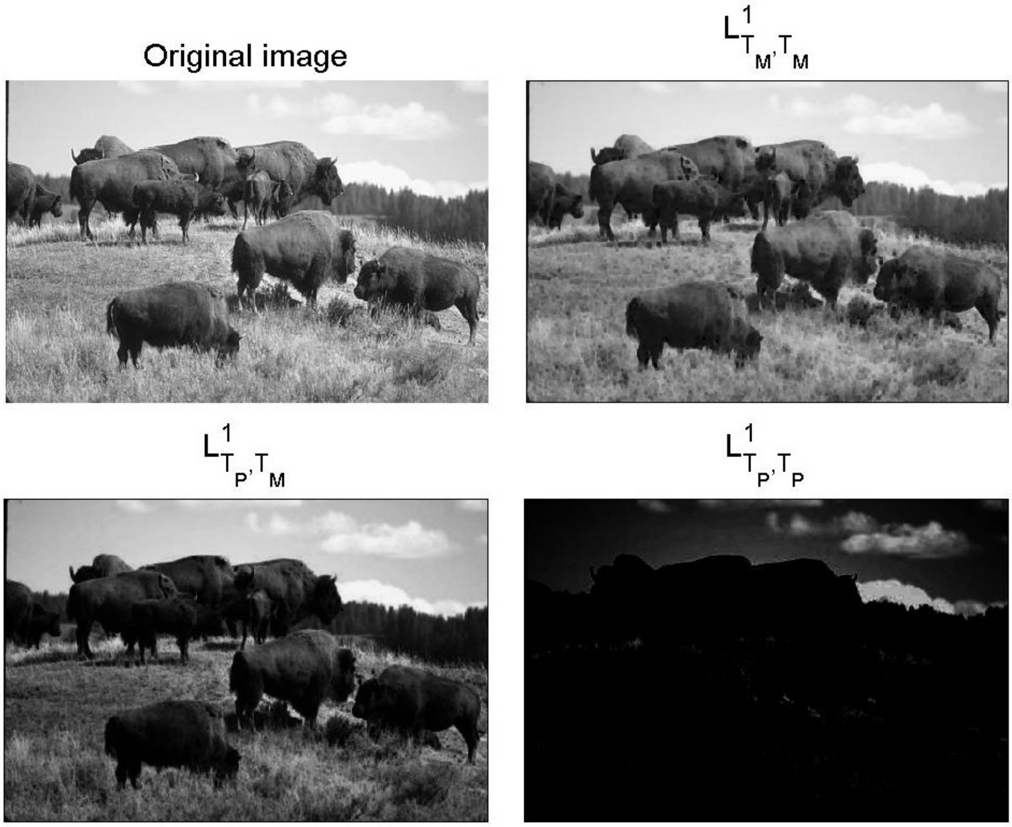

Figure 2: Comparative of lower constructors depending on different t-norms. T_P is the product t-norm and T_M the minimum.

For these three images (and also for the forthcoming) X-axis represents the different values of α, Y-axis contains the average over the 25 figures of the least square estimator (note that the lowest the error, the best the method). Finally, each line represents a different weighting method (average (A), equidistant method (E) and constant relation method with (C) $N = 2,3,4,5$ (C2, C3, C4, C5).

As it can be seen from the different figures, the best methods to obtain weights are the constant ones independently of the number of neighborhoods considered and the smoothing levels. In addition, it seems that the fuzzy image obtained using two neighborhoods has the lowest error. Regarding smoothing levels, the best are around 0.25.

When studying the behavior of the upper constructor (Figure 6) it is obtained exactly the same behavior. This situation remains when the behavior of the W-image is studied (see Figure 7). However, note that the error obtained by the approach based on the fuzzy image is the worst as the error obtained is the highest.

Therefore, let's analyze more in depth the behavior of the other two approaches. Figure 8 respectively shows the behavior of the best weighting method (C5) when 2, 3 or 4 neighborhoods are considered for upper and lower constructors.

X axis represents different α values and Y axis the value of the error. In boh cases, the configuration performing better is the one using two neighborhoods and $\alpha = 0.25$. In addition, as the lowest error is associated to the images produced by the upper constructor, it is possible to conclude that for this data set the best method to detect edges is the

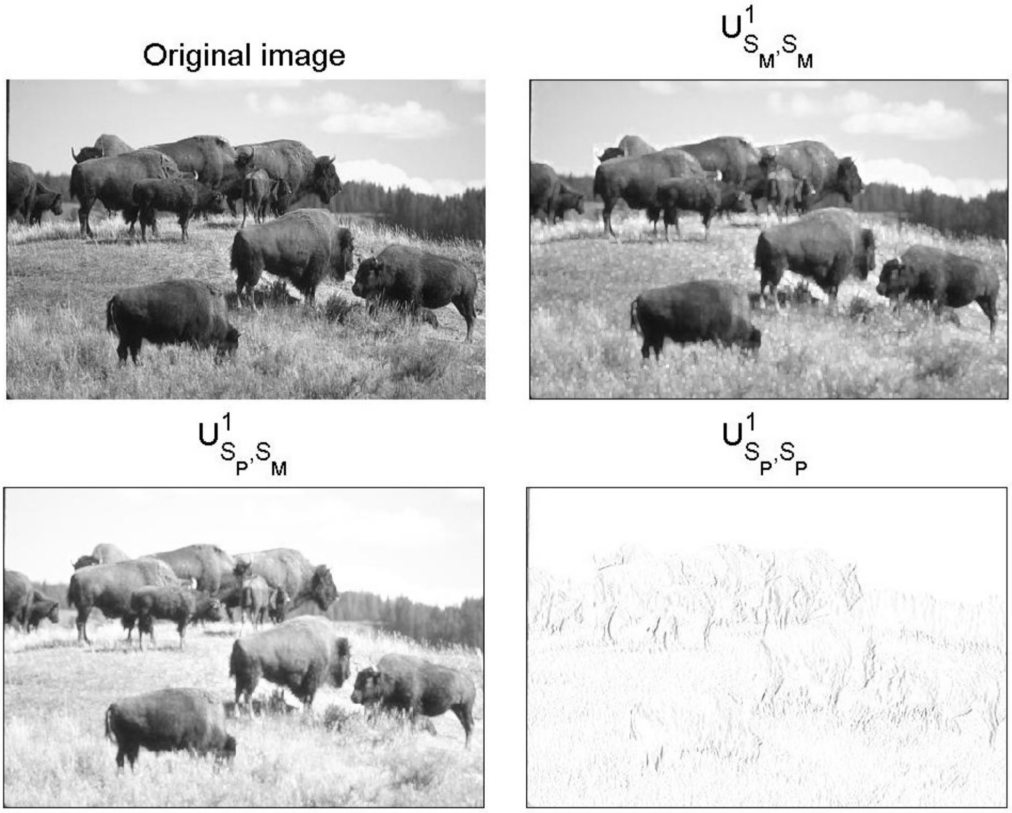

Figure 3: Comparative of lower constructors depending on the t-conorms. S_P is the probabilistic sum t-conorm and S_M the maximum

Figure 4: W-fuzzy images with $W[M,P] = U^{n,m}_{S_M,S_P} - L^{n,m}_{T_M,T_P}$.

one based on the upper constructor, weighting two neighborhoods with method C5 and $\alpha = 0.25$.

7. Final Remarks

This paper explores the links between FMM and IVFR. In addition different methods to construct

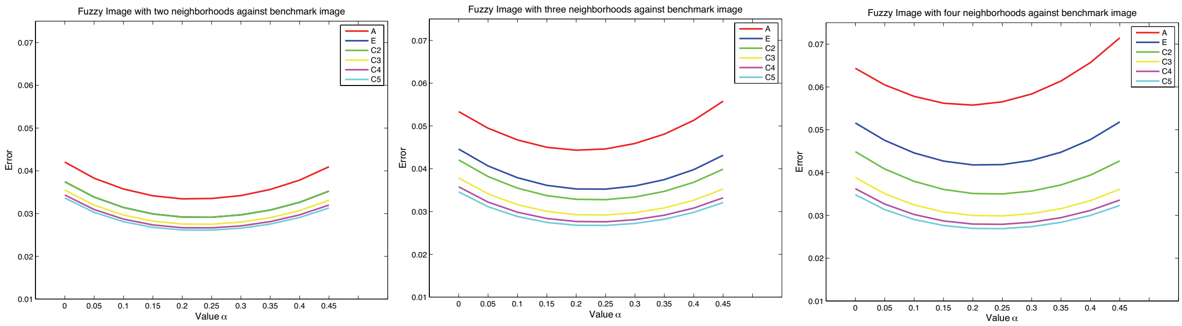

Figure 5: Performance of the lower constructor when 2 (left), 3 (middle) or 4 (right) neighborhoods are considered

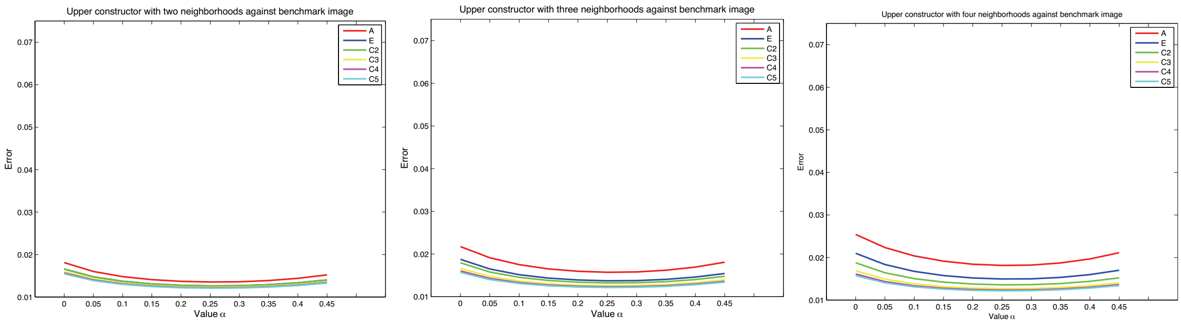

Figure 6: Performance of the upper constructor when 2 (left), 3 (middle) or 4 (right) neighborhoods are considered.

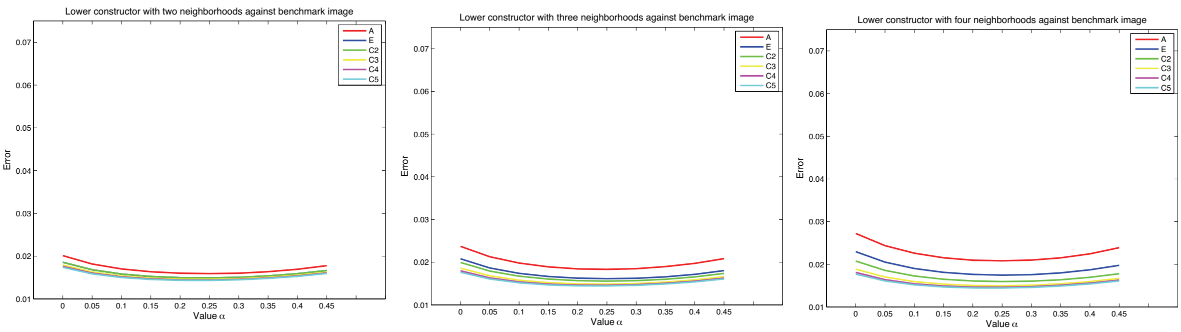

Figure 7: Performance of the lower constructor when 2 (left), 3 (middle) or 4 (right) neighborhoods are considered

IVFR are analyzed. Experimental results show that the best method for the studied images is the one based on the upper constructor. Considering weighting methods, the constant relation between consecutive weights is the one performing better. Regarding smoothing parameter, the best choice is $\alpha = 0.5$. These results suggest the importance of an adequate selection of parameters when these methods are applied to edge detection.

However, in order to set the optimal parametrization, it is necessary to make a more extensive experimentation, considering more images, in order to

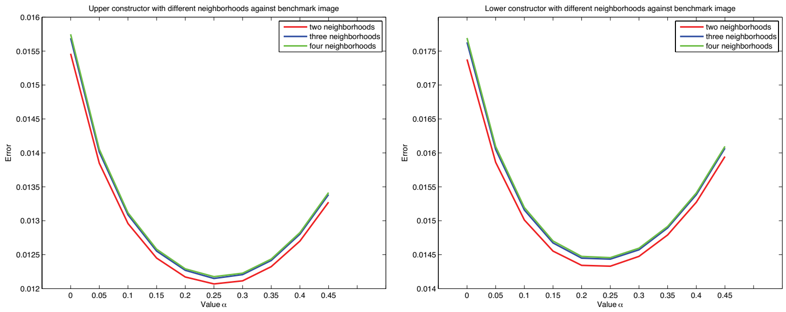

Figure 8: Upper (left) and Lower (right) constructors using $C5$ weighting method and $2,3$ and 4 neighborhoods.

check the right configuration. Therefore, as future work, we plan to consider a larger image database and to develop other IVFR construction methods.

Acknowledgements

This work has been partially supported by ERASMUS Mundus Project EUREKA SD 2013-2591 and by MINECO grant with reference TIN2014- 59543-P.

References

1. R. Wang, L. Gao, S. Yang and Y. Liu, *An Edge detection method by combining fuzzy logic and Neural networks* Machine Learning and Cybernetics **7** (2005), 4539–4543.
2. T. Hermosilla, E. Bermejo, A. Balaguer, and L.A. Ruiz, *Non linear fourth order image interpolation for subpixel edge detection and localization*, Journal on Image and Vision Computing **26** (2008), 1240–1248.
3. D. Marr and E. Hildreth, *Theory of edge detection*, Proceedings of the Royal Society of London (1980), 187–217.
4. D. Heric and D. Zazula *Combined edge detection using wavelet transform and signal registration* Journal of Image and Vision Computing **25** (2007), 652–662.
5. S. Konishi, A. L. Yuille, J. M. Coughlan, and S. C. Zhu, *Statistical Edge Detection: Learning and Evaluating Edge Cues*, IEEE Transactions On Pattern Analysis And Machine Intelligence **25(1)** (2003), 57–74.
6. R. González and R. Woods, *Digital Image Processing*, Addison Wesley, 2002.
7. J. Serra, *Image analysis and Mathematical Morphology, Vol. I.*, Academic Press, London, 1982.
8. J. Serra, *Image analysis and Mathematical Morphology, Vol. II.*, Academic Press, London, 1988.
9. B. De Baets, *Fuzzy morphology: a logical approach*, in: B.M. Ayyub, M.M. Gupta (Eds.), Uncertainty Analysis in Engineering and Sciences: Fuzzy Logic, Statistics, and Neural Network Approach, Kluwer Academic Publishers, Boston, 1997, 53–67.
10. L. Zadeh, *Similarity relations and fuzzy orderings*, Information Sciences **3** (1971), 177–200.
11. E. Barrrenechea, H. Bustince, B. De Baets, C. Lopez-Molina, *Construction of Interval-Valued Fuzzy Relations with application to the generation of fuzzy edge images*, IEEE Transactions on fuzzy systems **19** (2011), 819–830.
12. H. Bustince, E. Barrenechea, M. Pagola, J. Fernández, *Interval-valued fuzzy sets constructed from matrices: Application to edge detection*, Fuzzy Sets and Systems **160(13)**, (2009), 1819–1840.
13. P. Quirós, P. Alonso, I. Díaz, A. Jurío, and S. Montes, *An hybrid construction method based on weight functions to obtain interval-valued fuzzy relations*, Mathematical Methods in the Applied Sciencies, 2015, in press.
14. R. Sambuc, *Fonctions Φ-floues. Application l'Aide au Diagnostic en Patholologie Thyroidienne*, Ph. D. Thesis, Univ. Marseille (1975).
15. H. Bustince, *Interval-valued Fuzzy Sets in Soft Computing*, International Journal of Computational Intelligence Systems **3(2)** (2010), 215–222.
16. G. J. Klir, and B. Wheeler, *Fuzzy Sets and fuzzy logic*, Prentice Hall, New Jersey, 1995.
17. M. J. Frank, *On the simultaneous associativity of $F(x,y)$ and $x+y+F(x,y)$*, Aequationes Math **19** (1979), 194–226.
18. R. R. Yager, *On a general class of fuzzy connectives*, Fuzzy Sets and Systems **4** (1980), 235–242.
19. B. De Baets, E. Kerre, M. Gupta, *The Fundamentals of Fuzzy Mathematical Morphology, Part 1: Basic Concepts*, International Journal of General Systems **23** (1995), 155–171.

20. B. De Baets, E. Kerre, M. Gupta, *The Fundamentals of Fuzzy Mathematical Morphology. Part 2: Idempotence, Convexity and Decomposition*, International Journal of General Systems **23** (1995), 307–322.
21. I. Bloch and H. Maitre *Fuzzy Mathematical Morphologies: A Comparative Study* Pattern Recognition **28** (1995), 1341–1387.
22. V. Di Gesu, M. C. Maccarone, M. Tripiciano, *Mathematical Morphology based on Fuzzy Operators*, in: Fuzzy Logic, R. Lowen and M. Roubens, Eds., Kluwer Academic Publishers, 477-486 (1993).
23. E. Kerre, M. Nachtegael, *Fuzzy Techniques in Image Processing*, 52, New York (2000).
24. A. Bouchet, F. Benalczar Palacios, M. Brun and V.L. Ballarin, *Performance Analysis of Fuzzy Mathematical Morphology Operators on Noisy MRI*, Latin American Applied Research (LAAR), **44(3)** (2014), 231-236.
25. D. Martin, C. Fowlkes, D. Tal, J. Malik, *A Database of Human Segmented Natural Images and its Application to Evaluating Segmentation Algorithms and Measuring Ecological Statistics*, Proc. 8th Int'l Conf. Computer Vision **2** (2001), 416–423.